

# The Laser Welding with Hot Wire of 316LN Thick Plate Applied on ITER Correction Coil Case

Chao Fang · Yuntao Song · Weiyue Wu · Jing Wei ·  
Shuquan Zhang · Hongwei Li · N. Dolgetta ·  
P. Libeyre · C. Cormany · S. Sgobba

Published online: 30 July 2014  
© Springer Science+Business Media New York 2014

**Abstract** ITER correction coil (CC) cases have characteristics of small cross section, large dimensions, and complex structure. The cases are made of heavy thick (20 mm), high strength and high toughness austenitic stainless steel 316LN. The multi-pass laser welding with hot wire technology is used for the case closure welding, due to its low heat input and deformation. In order to evaluate the reliability of this welding technology, 20 mm welding samples with the same groove structure and welding depth as the cases were welded. High purity argon was used as the shielding gas to prevent oxidation because of the narrowness and depth of the weld. In this paper investigation of, microstructure characteristics and mechanical properties of welded joints using optimized welding parameters are presented. The results show that the base metal, fusion metal, and heat affected zone (HAZ) are all have fully austenitic microstructure, and that the grain size of fusion metal was finer than that of the base metal. The welding resulted in an increase of hardness in the fusion metal and HAZ. It was confirmed that the tensile strength of fusion metal was higher

than that of base metal and the impact toughness value is higher than industry standard requirement. Thus, this welding process was determined to be reliable for manufacture of the ITER CC cases manufacture.

**Keywords** Correction coils · Laser welding · Microstructure · Mechanical properties · Optimized

## Introduction

The correction coil (CC) is wound with CICC (Cable-in-Conduit Conductors) in the square 316L stainless steel jacket and wound into multiple pancakes embedded into coil cases. The CC cases shape is consistent with the coil shape, having characteristics of small cross section (168 mm × 147 mm), large dimensions (7 m), over a wide angle and large bending radius (12 m) [1]. The CC cases are made of high strength and high toughness austenitic stainless steel (316LN) hot rolled heavy plates. The case reinforces the winding packs against the electromagnetic loads at cryogenic temperatures, and minimizes stresses and deformations of the winding pack. The coil case is divided into two L-shaped parts for more convenient of the winding pack insertion. The overview of case and its cross-section are shown in Fig. 1.

The multi-pass laser welding with hot wire technology was selected for the case closure welding. The biggest advantage of the laser welding method is the small amount of heat input and small welding deformation. Hot wire is an additional heating wire process and it will increase the efficiency of the filler wire deposition. Multi-pass technology was chosen because of the 20 mm welding depth and to limit deformation. In addition, to obtain high strength and toughness for welded joints and to decrease welding

---

The views and opinions expressed herein do not necessarily reflect those of the ITER organization.

---

C. Fang (✉) · Y. Song · W. Wu · J. Wei · S. Zhang  
ASIPP, Shushan Hu Road 350, Hefei 230031, Anhui, China  
e-mail: fangchao@ipp.ac.cn

H. Li  
ITER China, 15B Fuxing Road, Beijing 100862, China

N. Dolgetta · P. Libeyre · C. Cormany  
ITER Organization, Route de Vinon sur Verdon,  
13115 St Paul lez Durance, France

S. Sgobba  
CERN, 1211 Geneva 23, Switzerland

**Fig. 1** Overview of CC case (a) and cross-section of case structure (b)

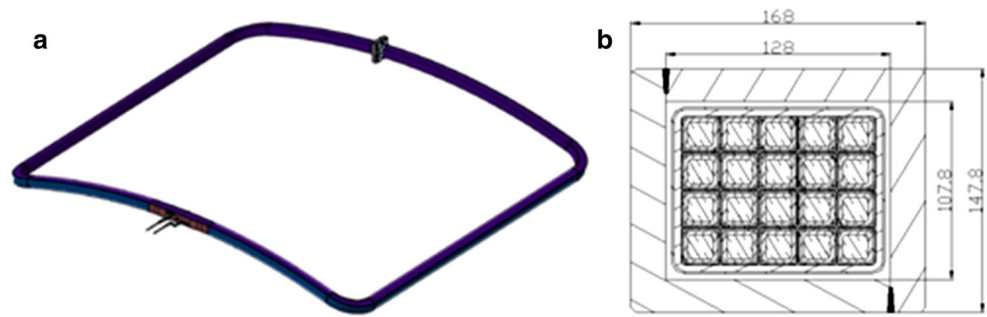


**Table 1** The chemical composition of 316LN stainless steel and wire (wt%)

Austenitic stainless steel 316LN									
C	Si	Mn	P	S	Cr	Mo	Ni	N	Cu
0.012	0.5	1.57	0.015	0.001	16.62	2.16	13.40	0.158	0.015
Ti	Nb	Al	V	Fe					
0.009	0.009	0.009	<0.01	Bal.					
Filler metal 316LMn for laser welding									
C	Si	Mn	P	S	Cr	Mo	Ni	N	Fe
0.018	0.46	7.01	0.017	0.003	20.59	2.83	15.37	0.156	Bal.

deformation 316LMn, which is fully austenitic stainless filler material, was used for the manufacturing development of the CC case. For ITER, the use of high-Mn content (6–10 %) welding filler is required for welding of 316LN. The high-Mn of filler metal is effective at preventing the formation of the ferritic phase at the weld region [2].

In actuality, the welding of CC cases is accomplished with two 20 mm thick weld with a V groove and root face. The weld is along the circumferential direction of the case and located on both sides of the case, the case will be turned over during the welding process. According to the joint structure of the case closure welding and standard ISO 15614-11, plate samples were made and tested to carry out the welding procedure qualification. Many experiments were done to optimize the welding parameters. Microstructure, hardness, tensile, and impact of the welded joint were investigated in order to know the weld quality and to confirm the reliability of the welding process.

**Experimental**

**Materials**

In the experiments, the base materials used for the welding were 316LN austenitic stainless steel plates with 20 mm thickness. The welding wire used was 316LMn with a 1.2 mm diameter. The dimensions of the completed laser welded samples are 300 mm × 300 mm × 20 mm (thickness). The chemical composition (wt%) of base and filler metal are summarized in Table 1.

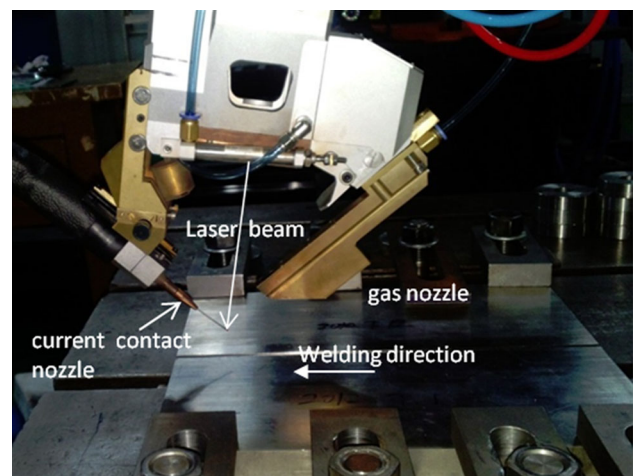


**Fig. 2** system of welding head, filler wire (left) and gas nozzle (right)

**Laser Welding**

The laser welding with hot wire technology was carried out using the TS5000 hot wire feeder system (Fronius) and the YLS-4000 fiber laser (IPG) which has the features of continuous wave and no beam oscillation. A special laser welding head, which was designed for the system, was mounted on the KUKA KR60HA robot arm. The setup of the welding head, geometry of filler wire feeder and gas nozzle can be seen in Fig. 2 [3]. The laser spot is located in the middle of weld and coincides with the top point of wire during the welding process. High purity argon (99.999 %) is used as shielding gas.

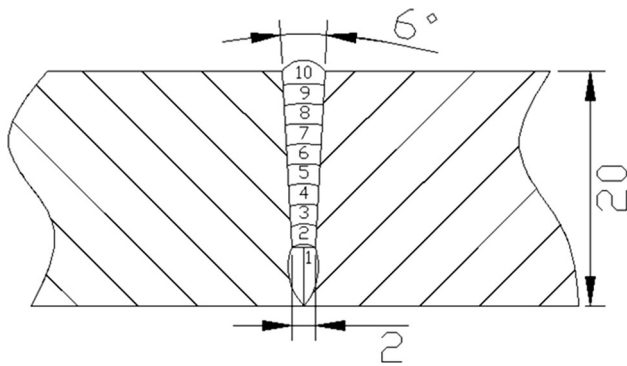


**Fig. 3** Welding joint

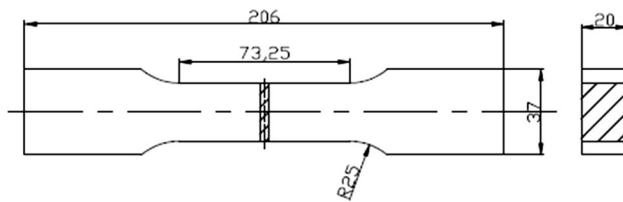


**Fig. 4** Dimension of tensile specimen (mm)

was used as a shielding gas to prevent oxidation (15–20 L/min). In the experiments, the configuration of the joint groove was V shaped and the weld was completed in ten passes as shown in Fig. 3 (layer 10 is the cosmetic layer). The welding scheme is a 5 mm deep root pass, followed by nine layers to fill the remaining 15 mm and completed in this way the 20 mm thick weld. During the welding process, an angle grinder was used to grind the weld for facilitating the welding of the next layer and removing surface oxide. Also the interlayer-temperature was controlled and kept below 100 °C to reduce hot cracking sensitivity.

#### Test Procedure

The specimens for the metallurgical and mechanical tests were sampled from the welded joints. The welds were chemically etched for observation of the microstructure using optical microscopy. According to the international standard EN ISO9015-1, hardness distribution at various positions on the welded joint was measured using a Vickers hardness tester, with a testing load of 10 kg. The tensile and impact properties of the specimens were tested based on the international standards EN ISO4136:2011 and ISO9016:2012, respectively. Dimensions of standard tensile and impact specimens are shown in Figs. 4 and 5. Tensile tests of two specimens were carried out at room temperature with the weld located at the center of the specimens. There were six impact specimens divided into two groups of three: one group of specimens with their

notch located in the weld metal, and the second with their notch located in the heat affected zone (HAZ) (1 mm from fusion line). The impact tests were carried out at 4.2 K and the axis of V-notch for each impact specimens was perpendicular to the surface of welded plate.

## Results and Discussion

### Welding Process Parameters Optimization

In order to achieve the requirements of case welding, many experiments were done to optimize the welding process parameters. The optimized parameters included the root pass parameter and the cosmetic parameters.

Generally, there is no filling wire within the laser welding of root pass of plate. However, because of the large dimensions and complex structure of CC case, a certain amount of root gap would appear after case assembly. The laser energy would be lost without filling wire, and this would affect the mechanical integrity and electrical performance of the insulation material inside the case. As a result, filling wire was also used during the root pass welding.

It was found that there was good fusion between each layer and no incomplete fusion in the sidewall of layers 1–9 (according to Fig. 3) during the welding experiments. However, incomplete fusion of the cosmetic layer, which used the previous layers welding parameters, was observed. This was due to the V shaped groove, the cosmetic layer is wider than the previous layers and the bead width based on the previous layers welding parameter was not wide enough. This resulted in incomplete fusion of cosmetic layer. Therefore, it was necessary to increase the weld width to match the groove width. In order to increase the weld width, a larger defocusing distance was used to achieve the bigger spot diameter to form a larger weld crater. Moreover, a slower welding speed was used to increase the welding heat. The bead width, using the new cosmetic parameter, had a larger surplus compared with groove width. The optimized cosmetic welding parameter effectively eliminated incomplete fusion. The weld surface appearances of old and new cosmetic layers are shown in Figs. 6 and 7. It was observed that there was incomplete fusion in Fig. 6 and defect-free weld in Fig. 7.

The corresponding welding parameters were chosen and shown in Table 2.

### Microstructure Observation and Hardness Tests

The microstructure of the base metal, HAZ and the fusion metal are shown in Fig. 8. It was observed that the base metal, HAZ and the fusion metal had a fully austenitic

**Fig. 5** Dimension of impact specimen (mm)

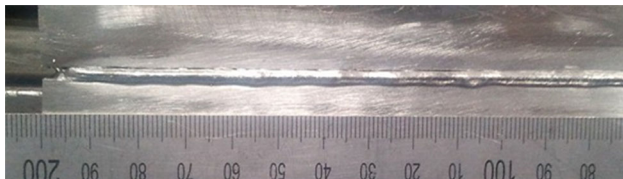
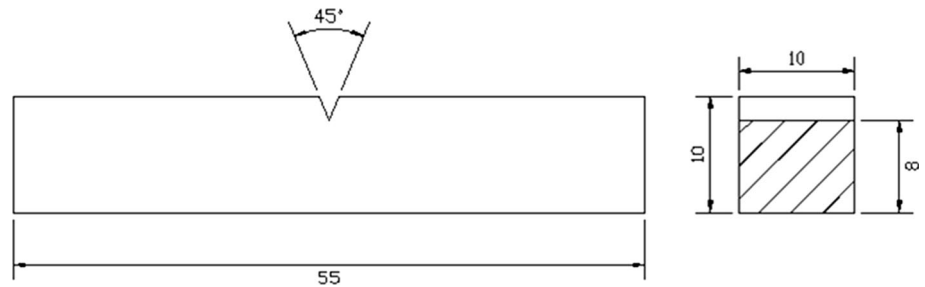


**Fig. 6** The weld surface based on the old cosmetic welding parameter



**Fig. 7** The weld surface based on the new cosmetic welding parameter

**Table 2** Welding parameters in the experiment

Layer	Laser power (KW)	Defocusing distance (mm)	Welding speed (cm/min)	Wire current (A)
1	3.5	+5	100	250
2-9	3.8	+25	150	250
10 (old)	3.8	+25	150	250
10 (new)	3.9	+45	60	250

microstructure, and the base metal recrystallized by the solution treatment processing, displayed uniform equiaxed grains of austenite microstructure. By careful examination of the micrographs, it was revealed that mainly cellulars and dendrite grains were formed in the fusion metal. The weld metal formed with these grains perpendicular to the fusion line and growth to the weld center. This is the typical characteristic of the primary austenitic solidification. In addition, the ferrite-forming elements Cr and Mo were segregated at boundaries of cellulars and dendrites based on the primary austenitic solidification to generating the black grains in the Fig. 8c. It is well known that the

solidification model depends on the ratio of the Cr and Ni, and the primary austenitic solidification was expected since the ratio of the chromium equivalent and nickel equivalent was less than 1.5 [4] [5] [6]. So, no  $\delta$ -ferrite was detected in the laser welded steel. The grain size of fusion metal was finer than that of base metal and the grain size of HAZ did not grow obviously as the result of rapid solidification and alloying elements. Laser welding of high cooling rate is conducive to grain refinement. And a base material which contains a small amount of Ti, V, Al, Nb and other alloying elements will have a high melting point and the inappropriate growing of nitride and carbide, which have the characteristic of small grains and dispersed small grains, will hinder grain growth.

No obvious surface and internal defects were found by means of the nondestructive examinations (radiographic and penetration testing). And the magnetic permeability measurement result shows the value measured is lower than 1.03 which has reached the requirements of design [7]. The macrograph and Vickers hardness distribution of the welded joints are shown in Fig. 9. The weld metal can be clearly seen in the welded joint (see Fig. 9 a). The trends of the hardness variation is shown in Fig. 9b, c. The locations for measurements are also depicted in Fig. 9a: line A located at 2 mm from the top surface of the welded plate and line B located at 2 mm from the bottom surface of the welded plate. It can be seen that the top and bottom weld hardness values were consistent the Fig. 9b, c. The maximum hardness was in the HAZ zone, 228 HV (top line) and 217 HV (bottom line). The minimum hardness was located in the base metal, 152 HV (top line) and 150 HV (bottom line). The characteristics of hardness distribution were essentially determined by the microstructure of the various zones, owing to their different welding thermal cycles during welding. Such hardness profiles are considered to be associated with the high cooling rates from the liquid state that lead to the formation of microstructure and fine grains in the fusion metal [8]. Furthermore, the HAZ zone must have the secondary phase precipitates which will result in higher hardness of HAZ. This is because of the HAZ zone was heated to the temperature of the alloy solidus during the welding. Many precipitates of the base metal may be



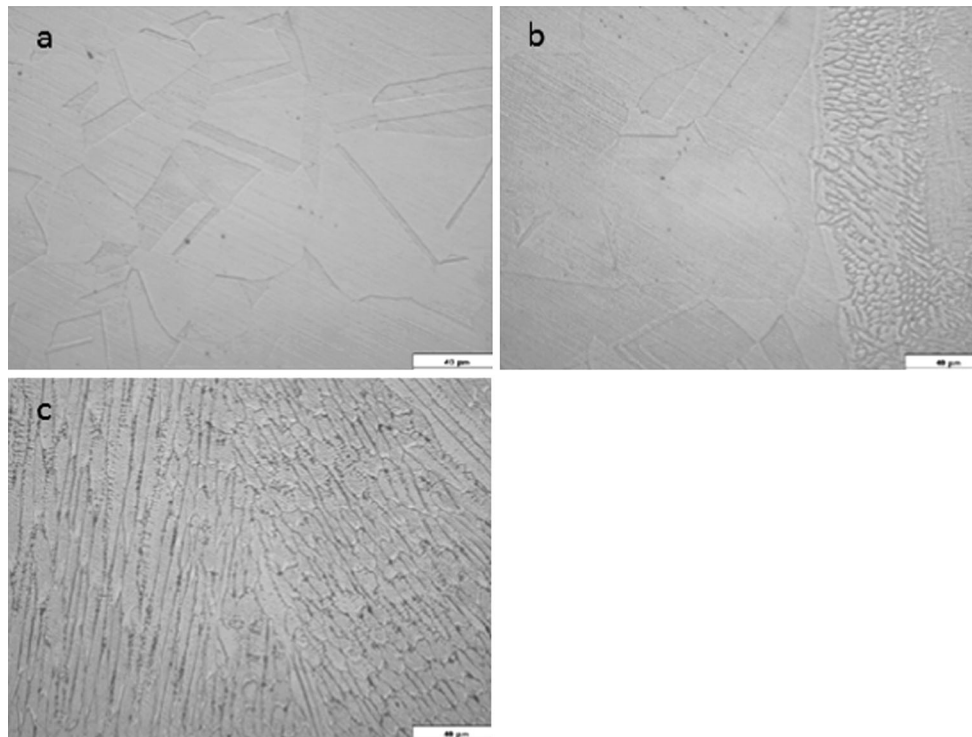


**Fig. 8** The optical microstructures of base metal (a), HAZ (b) and fusion metal (c) in welded joint

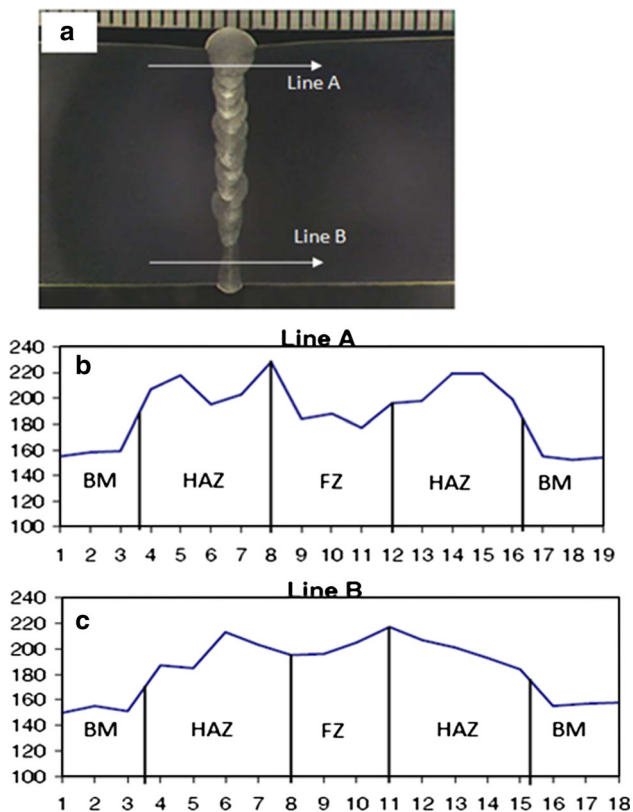


**Fig. 9** Vickers hardness distribution in the cross-welded joint: **a** macrograph of the welded joint; **b** hardness distribution measured along *top line*; **c** hardness distribution measured along *bottom line*

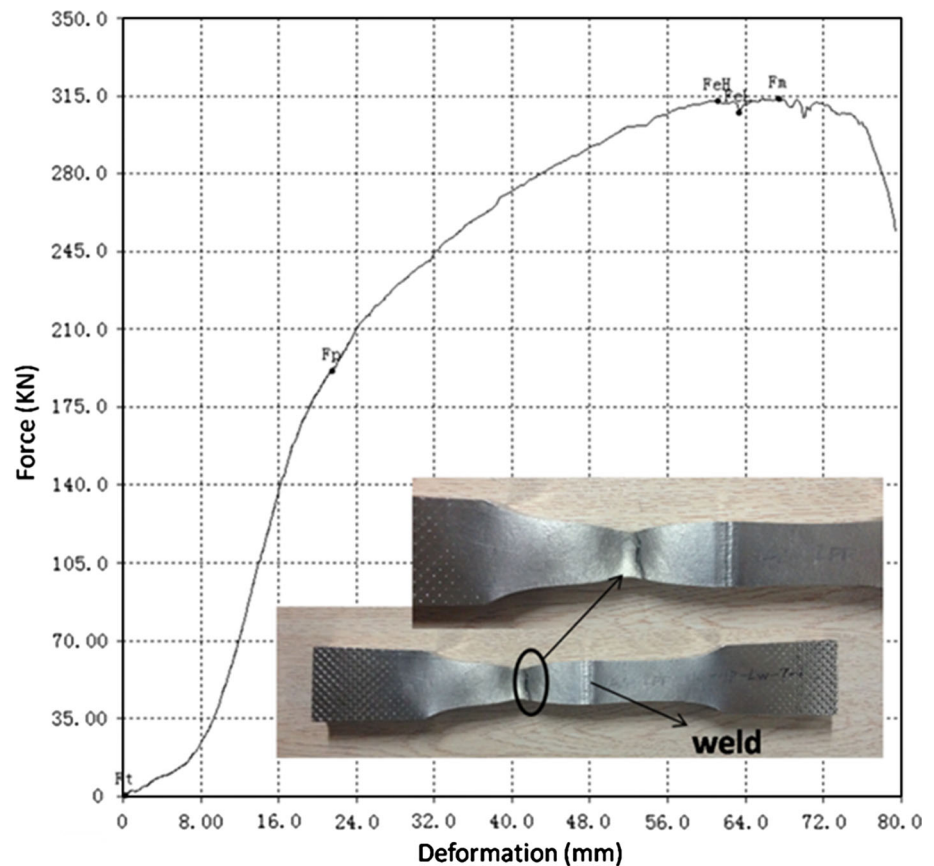
dissolve which will result in supersaturation during cooling and generating precipitates of carbides and nitrides [5].

#### Tensile Tests and Charpy Impact Test

The tensile strength of the two welded joints specimens, which were up to 632 MPa and 646 MPa, reached the design requirement at room temperature ( $>480$  MPa) [7]. Figure 10 shows the photograph of one broken specimen after tensile testing and the force-deformation curve. It was found that all tensile specimens were fractured in the base metal zone and the welded joint had significant plastic deformation before fracture. This confirmed the fact that the tensile strength of the welded joint was higher than that of the base metal and the welded joint had good ductility. This result indicates the welding procedure of the experiment is quite reasonable.

The Charpy-V notch-impact tests were done at 4.2 K. The results show that the notch-impact toughness value of weld metal was  $257 \text{ J/cm}^2$ , while the notch-impact toughness value of HAZ was  $86 \text{ J/cm}^2$ . The average impact toughness value of weld metal and HAZ were higher than Chinese industrial standards ( $>37 \text{ J/cm}^2$ ) [9], so the impact strength of the welded joint was qualified. Obviously, the impact toughness of HAZ was far less than that of weld metal. It was mainly caused by the grain size of notch-impact specimens. The notches of the weld metal impact tests specimens were located the weld center where the

**Fig. 10** Force-deformation curve of tensile test and broken specimen



grain was finer than that of HAZ. Moreover the secondary phase precipitates in the HAZ which will result in lower toughness and easier brittle fracture. So, the impact toughness value of HAZ was far less than that of weld metal.

## Conclusion

1. 20 mm standard sample was designed to carry out the welding procedure qualification of the CC case closure welding. Multi-pass laser welding with hot wire technology was successfully used on these standard samples with optimized welding parameters, where the welded joint was full penetrated and free of macro defects.
2. It was observed that the base metal, fusion metal and HAZ had a fully austenitic microstructure, which is the typical characteristic of the primary austenitic solidification. The grain size of fusion metal was finer than those of base metal and grain size of HAZ did not grow obviously as the result of rapid solidification and alloying elements.
3. The maximum hardness was located in HAZ, the fusion metal and HAZ hardness value was higher than the base metal.

4. The laser welded joints had good mechanical properties of toughness and ductility. The tensile strength of the welded joint was higher than that of the base metal, this was mainly caused by the grain refinement. Results of Charpy-V notch-impact tests displayed that the impact toughness value was far higher than the industry standard requirements. Further efforts will focus on the washer, bolt, rail and joint; the feeder will also be included.

**Acknowledgments** The authors would like to acknowledge the ITER IO magnet division for their contribution to the definition of CC technical specification and development of task packages. We also thank Beijing University of Technology and SIASUN for their contributions on the equipment and welding technology of CC case.

## References

1. Z. Zhou et al., Research on manufacture and enclosure welding of ITER correction coils cases. *IEEE Trans. Appl. Supercond* **22**, 3 (2012)
2. H.C. Kim, K. Kim, Y.S. Lee, S.Y. Cho, H. Nakajima, Study on the weld characteristics of 316LN by magnetization measurement. *J. Nuclear Mater.* **386–388**, 650–653 (2009)
3. Tommi Jokinen et al., High power Nd:YAG laser welding in manufacturing of vacuum vessel of fusion reactor. *Fusion Eng. Des.* **69**, 349–353 (2003)

4. J.A. Brooks, M.I. Bakes, L.A. Boatner, *Metall. Trans.* **22A**, 915 (1991)
5. J.C Lippold, D.J Kotecki, *Welding Metallurgy and Weldability of Stainless Steels* (Wiley, Hoboken, 2005)
6. V. Shankar, T.P.S. Gill, S.L. Mannan, S. Sundarlsan, Solidification cracking in austenitics stainless steel welds. *Sadhana* **28**(2–4), 359–382 (2003)
7. ITER Design Description Document, Magnets DDD 11 ITER\_D\_2N6NUK v1.13, 5. CC Coils and Structures. Sept 2009
8. S.C. Tjong, S.M. Zhu, N.J. Ho, H.S. Ku, Microstructural characteristics and creep rupture behavior of electron beam and laser welded AISI 316L stainless steel. *J. Nucl. Mater.* **227**, 24–31 (1995)
9. Chinese industrial Standards NB/T 47014-2011, Welding procedure qualification for pressure equipment